ORIGINAL ARTICLE

Relationship of renal apparent diffusion coefficient and functional MR urography in children with pelvicalyceal dilation

Maria A. Bedoya [1,2] · Jeffrey I. Berman [1,2] · Jorge Delgado [1] · Dmitry Khrichenko [1] · Christian A. Barrera [1] · Robert H. Carson [1] · Kassa Darge [1,2]

Abstract

Objective The aim is to evaluate the age-related changes and relationship of renal apparent diffusion coefficient (ADC) against the morphological and functional changes detected by functional magnetic resonance urography (fMRU) in children with pelvicalyceal dilation, with suspected or known ureteropelvic junction obstruction.

Materials and methods We retrospectively analyzed fMRUs with diffusion-weighted imaging (DWI) of the kidney in 35 subjects (25 males; median age: 7.1 years, range: 0.3–22.7 years) with 70 kidneys (40 with pelvicalyceal dilation and 30 with no pelvicalyceal dilation). Inclusion criteria were pelvicalyceal dilation, the absence of duplex kidneys and no ureteric dilation. DWI was performed with 3 diffusion gradient directions (b values = 0, 200, 500, 800 and 1,000 s/mm2). Metrics for fMRU included calyceal and renal transit times (CTT, RTT), time-to-peak (TTP), differential renal function based on volume (vDRF), Patlak number (pDRF) and combined volume and Patlak number (vpDRF). The grades of pelvicalyceal dilation, cortical thinning and corticomedullary differentiation were evaluated. The relationship between ADC values and the fMRU parameters was analyzed.

Results ADC increases with age in kidneys without pelvicalyceal dilation (R^2=0.37, $P<0.001$). Renal ADC does not correlate with any of the morphological or fMRU parameters ($P>0.07$). The median ADC of kidneys without pelvicalyceal dilation was 3.73×10^{-3} mm^2/s (range: $2.78–5.37\times0^{-3}$ mm^2/s) and the median ADC of kidneys with pelvicalyceal dilation was 3.82×10^{-3} mm^2/s (range: $2.70–5.70\times10^{-3}$ mm^2/s). There was no correlation between ADC and the absolute differences of vDRF or pDRF ($P>0.33$).

Conclusion Renal ADC does not correlate with morphological and functional results of fMRU changes in children with pelvicalyceal dilation due to suspected or known ureteropelvic junction obstruction.

Keywords Apparent diffusion coefficient · Children · Diffusion-weighted imaging · Dilation · Kidney · Magnetic resonance imaging · Urography

Introduction

Excretory urography and renal scintigraphy are the conventional methods for evaluating renal excretion and function. However, their use in children is limited because of their radiation exposure and low resolution. Functional magnetic resonance urography (fMRU) is the current standard to evaluate the urinary tract in children. fMRU lacks radiation, has high spatial resolution and provides comprehensive morphological and functional evaluation. However, fMRU results require careful interpretation in cases of pelvicalyceal dilation, as we lack absolute cutoffs for the fMRU parameters to determine cases that require surgery or predict the outcome after surgery. Diffusion-weighted imaging (DWI) measures the random motion of water molecules, which can be free or restricted by cellular membranes or other barriers. Apparent diffusion coefficient (ADC) is a quantitative parameter that measures the directionally averaged magnitude of diffusivity. ADC

✉ Maria A. Bedoya
bedoyam@email.chop.edu

1. Department of Radiology, The Children's Hospital of Philadelphia, 34th Street and Civic Center Boulevard, Philadelphia, PA 19104, USA

2. Perelman School of Medicine, University of Pennsylvania, Philadelphia, PA, USA

provides microstructural information about tissue microstructure by using the movement of water to probe extracellular and intracellular extravascular spaces [1].

Currently, the most extensive application of DWI is in neuroimaging. In recent years, the clinical use of DWI in extracranial organs, such as the kidneys, increased with the development of faster imaging sequences (echoplanar and parallel imaging), use of phased-array multichannel surface coils and stronger diffusion gradients [2, 3]. Kidneys are one of the most interesting organs to evaluate water diffusion because of their function in water filtration, absorption and secretion. DWI has been proven to be clinically useful in the characterization of renal tumors [4–7], diagnosis and follow-up of pyelonephritis [8–10], and evaluation of parenchymal diseases [11] and acute renal transplant dysfunction [12].

The postnatal kidney undergoes complex maturation of physiology and anatomy. Renal ADC values increase with age, particularly during the first year of life [13, 14]. Based on studies performed in adults, renal ADC correlates with renal function, especially with the glomerular filtration rate (GFR). ADC values may be useful to evaluate functional status of kidneys with hydronephrosis [15, 16], chronic renal failure [11, 17–19] and renal artery stenosis [18]. However, the use of renal ADC values as a potential biomarker for renal function has not been adequately validated. Studies show renal parenchymal ADC values do not change in acute obstructed kidneys in comparison to contralateral normal kidneys [20]. More importantly, there are few publications demonstrating the correlation between ADC and renal function or morphology in children [21–23]. The primary purpose of this study is to evaluate the renal ADC age-related changes and the relationship between renal ADC against the morphological and functional changes detected by fMRU in children with pelvicalyceal dilation, with suspected or known ureteropelvic junction (UPJ) obstruction.

Materials and methods

Patients

This study was approved by the institutional review board (IRB) of our hospital, and was performed in compliance with the Health Insurance Portability and Accountability Act (HIPAA). The requirement for informed consent was waived. A DWI sequence is part of our institutional fMRU protocol with the primary aim of improved detection and characterization of incidental renal lesions. We retrospectively reviewed all renal DWI sequences performed over a period of 3 years. The inclusion criteria were complete fMRU exam, the presence of unilateral or bilateral pelvicalyceal dilation suggestive of UPJ obstruction (pelvicalyceal dilation without ureteral dilation), pre-scan administration of furosemide and intravenous

hydration, axial DWI of the kidneys performed on 1.5-T magnets and the availability of functional data. This search yielded 110 subjects. Exclusion criteria included suboptimal overlap of fMRU post-contrast dynamic scans and DWI segmentations due to motion artifacts (n=37), presence of duplex kidneys (n=30), renal tumors (n=2) and suboptimal DWI sequences (n=6). The exclusion criteria were set to decrease the likelihood of inappropriate placement of the regions of interest (ROIs) as they are potential limitations to reliable segmentation of the renal parenchyma. Inclusion criteria were met by 35 subjects (10 girls and 25 boys; median age: 7.1 years, age range: 0.3–22.7 years) with 30 kidneys without pelvicalyceal dilation and 40 kidneys with pelvicalyceal dilation. Among the patients included in the study, the main indications of the fMRU were hydronephrosis and postsurgical UPJ obstruction follow-up.

fMRU scan

fMRU images were acquired on a 1.5-T scanner (Avanto; Siemens Healthcare, Erlangen, Germany) with a 6-channel phased-array body matrix coil in combination with a 24-channel spine coil. Children younger than 7 years (n=17) were sedated using a combination of 0.1 mg/kg of midazolam, 0.1 mg/kg of fentanyl and 3 mg/kg of pentobarbital. All fMRU images were acquired using the standard institutional fMRU protocol. All children were hydrated with 20 cc/kg of normal saline (0.9%) infused over 30–40 min before scanning. Furosemide (Lasix; Sanofi-Aventis, Paris, France) at 1 mg/kg (maximum: 20 mg) was administered intravenously 15 min before intravenous injection of gadolinium-diethylenetriamine penta-acetic acid (DTPA) (Magnevist; Bayer-Schering, Berlin, Germany) at a dose of 0.2 mmol/kg. Pre-contrast images included sagittal T2 half-Fourier RARE (rapid acquisition with relaxation enhancement) acquisition (HASTE [half-Fourier acquired single-shot turbo spin echo]) (repetition time [TR]/echo time [TE], 1,100/99 ms; thickness, 3 mm; matrix, 256×202), axial and coronal high-spatial resolution fat-saturated T2 turbo spin echo with motion reduction (BLADE) (TR/TE, 6,000/102–145 ms; thickness, 3 mm; matrix, 320×320), coronal T1 gradient-echo sequence (TR/TE 240/4.5 ms; thickness, 3 mm; matrix, 256×202), coronal three-dimensional [3-D] T2 with fat saturation (SPACE [sampling perfection with application optimized contrasts using different flip angle evolution]) (TR/TE, 1,800/599 ms; thickness, 1 mm; matrix, 384×357), and coronal 3-D T1 gradient recalled echo (GRE) with fat saturation VIBE (volumetric interpolated breath-hold examination) (TR/TE, 3.63/1.23; thickness, 2 mm; matrix, 256×168). Post-contrast MR images were acquired for the functional analysis using a 3-D fat-suppressed T1-weighted gradient-echo sequence (VIBE) (TR/TE, 3.63–4.24/1.12–1.31 ms; flip angle, 30°; thickness, 2-3 mm based on body size; no gap or overlap between slices; matrix,

256×1,680). Functional dynamic images were repeated 55 times over a 15-min period with increasing pauses between acquisitions. We obtained additional delayed post-contrast images in the prone position when contrast excretion was not visualized in one or more ureters during the dynamic images.

fMRU analysis

fMRU post-processing The renal segmentation of the functional analysis was performed by a research fellow (D.K.) with 10 years of experience using the Children's Hospital of Philadelphia (CHOP)-fMRU software, which is written in Interactive Data Language (Harris, Boulder, CO). This software is available freely online (www.CHOP-fMRU.com) [24]. Regions of interest (ROIs) were placed in the whole renal parenchyma of the right and left kidney, including the renal cortex and medulla. The pelvicalyces were not included in the parenchymal fMRU ROIs. Calyceal transit time (CTT) represents the time needed in seconds for the contrast agent to reach the calyces once it is depicted in the aorta. Renal transit time (RTT) is the time needed in seconds for the contrast agent to reach the ureter, below the level of the lower pole of the kidney; it is influenced by patient position, position of the pelviureteric junction and extent of pelvicalyceal dilation. In kidneys without excretion, the CTT and RTT are automatically calculated as the time of the last delayed image [25]. Time-to-peak (TTP) represents the time in seconds to reach maximal parenchymal enhancement. Volumetric differential renal function (vDRF) is the split percentage of the renal function based on the enhancing renal parenchymal volumes. Patlak differential renal function (pDRF) is the split percentage of the renal function based on the generated Patlak numbers, a potential indicator of the glomerular filtration rate (GFR) [24]. Differential renal functions are expressed for each kidney as the percentage of relative volume or function to the overall renal function of a subject. The absolute Patlak numbers are calculated in order to generate the pDRF and combined volumetric and Patlak DRF (vpDRF) as a percentage [24]. All these parameters were exported from the clinical fMRU data. We calculated the difference between RTT and CTT for each kidney (RTT-CTT) as an indicator of dilation and excretion in seconds. Excluding the subjects with bilateral dilation, we calculated the absolute difference in vDRF and pDRF between the normal and the dilated kidney in each subject.

Qualitative analysis of the fMRU Qualitative morphological analyses were performed by a physician radiologist (K.D.) with more than 20 years of experience in pediatric imaging of the genitourinary system, as follows:

> *Pelvicalyceal dilation:* We evaluated qualitatively the presence of pelvicalyceal dilation of each kidney using the axial high-spatial resolution fat-saturated T2 and the

coronal 3-D T2 with fat-saturation sequences. We used the US grading of pelvicalyceal dilation by Riccabona et al. [26] and as previously reported by Delgado et al. [27]. This classification encompasses a six-grade scale, from 0 (no pelvicalyceal dilation) to 5 (severe dilation). Grades 0 and 1–2 were considered no or no significant dilation with normal forniceal shape. Grade 3 had pelvic dilation with reduced forniceal and papillary differentiation. Grade 4 was the same as Grade 3 plus cortical thinning. Grade 5 was marked dilation with severe cortical thinning (membrane-like parenchyma) and loss of pelvicalyceal configuration. For statistical purposes, Grades 0 and 1–2 were considered to have no pelvicalyceal dilation, and Grades 3 to 5 were considered to have pelvicalyceal dilation

Pelvic and calyceal anteroposterior (AP) diameter: On the axial high-spatial resolution fat-saturated T2 sequences, we measured the AP diameter (in mm) of the intrarenal pelvis and the largest calyx of each kidney.

Corticomedullary differentiation: We evaluated the corticomedullary differentiation, on the pre-contrast images, as normal or decreased.

Cortical thinning: We used all the images of the fMRU study to evaluate cortical thinning of each kidney. A 4-point scale was used as follows: 1=no cortical thinning, 2=mild cortical thinning, 3=moderate cortical thinning and 4=severe (membrane-like) cortical thinning.

Renal enhancement: We used the nephrogram of the dynamic images, delayed post-contrast images and the renal enhancement curves of the post-processing analysis to evaluate the renal enhancement of each kidney [24]. A 3-point scale was used. Grade 1=normal, when normal changes in the signal intensity of the nephrogram and the enhancement curves were seen. In subjects with unilateral UPJ obstruction, the renal enhancement and curves were symmetrical. Grade 2=decreased, when there was a delayed or dense nephrogram with abnormal peak on the enhancement curves. In unilateral UPJ obstruction, the dilated kidney had an asymmetrical enhancement on the nephrogram with a delayed peak compared to the normal kidney. Grade 3=absent, when there was a complete absence of renal enhancement on the post-contrast dynamic series and delayed images.

Excretion: We used the post-contrast dynamic images and the delayed images to evaluate the excretion of each kidney. A 4-point scale was used. Grade 1=normal, when the visualization of the contrast in the ureter was rapid. In subjects with unilateral UPJ obstruction, the excretion was symmetrical between the kidney without and with dilated pelvicalyces. Grade 2=decreased, not clinically relevant delay of contrast excretion; the ureter filled with contrast was visible on the dynamic images. Grade 3=decreased, clinically relevant significant delay in the

contrast excretion and the contrast in the ureter was not visible on the dynamic images, but later on the delayed images. Grade 4=absent excretion, a contrasted ureter was not visible on the delayed images.

DWI scans and image analysis

Renal DWI was a free-breathing single-shot spin-echo echoplanar sequence in the axial plane with TR/TE, 3,500-4,700/73–108; bandwidth, 965 Hz per pixel; echo train length 0.47 ms, field of view, 384 mm at 100%; section thickness, 4–7 mm; intersection gap, 0.4–0.7 mm; and matrix size, 128×128 mm with a 100% phase resolution and without interpolation of the acquisition. The median voxel volume was 10.01 mm^3 (7.6–34.9 mm^3). Fat saturation was used to avoid chemical shift artifacts. No oversampling or zoom technique were used. A 3-directional diffusion-weighting gradient was applied with b-values of 0, 200, 500, 800 and 1,000 s/mm^2, 3 averages and a parallel imaging factor of 2. The average time of acquisition was 1 min, varying based on the number of slices.

ROIs of each renal parenchyma from the clinical fMRU analysis were loaded semiautomatically over the DWI data (Fig. 1). The ROI pixel coordinates from the fMRU analysis file were converted into spatial coordinates using the slice position and slice orientation DICOM (Digital Imaging and Communications in Medicine) tags from the fMRU scan. These coordinates were converted back into pixel coordinates, but this time using slice position and slice orientation DICOM tags from the DWI sequence. Image overlays were created and evaluated by a postdoctoral research fellow with 2 years of radiology experience for accuracy of the overlays. The ROI position was evaluated on a 2-point scale: Grade 1=excellent ROI position of the right and left kidney and Grade 2=suboptimal overlap of fMRU and DWI segmentations due to patient motion between the functional and DWI sequences. As previously stated, 37 cases with suboptimal position of the renal ROIs were excluded.

ROIs were placed on the whole renal parenchyma as the ADC maps were heterogeneous and it was not possible to differentiate reliably the cortex and medulla in younger children.

ADC maps were calculated from the DWI images with b-values of 0, 200, 500, 800 and 1,000 s/mm^2 using a mono-exponential decay model with the following formula:

$$S(b) = S(0) \times e^{-ADC \times b} + C$$

Where S(b) is signal intensity at b-value=b, S(0) is signal intensity at b-value=0, and C is the noise plateau [28, 29].

Statistical analysis

All analyses were performed using SPSS statistical software (version 21.0.0, IBM; Armonk, NY). Each kidney unit was treated as an independent unit. The Shapiro-Wilk test was used to evaluate the distribution of the data. Linear regression of ADC values and age was performed to determine the association of ADC and age. To assess the correlation of ADC values and fMRU parameters, hierarchical regressions were performed with ADC values as the dependent variable and age entered first and fMRU parameter second. The fMRU parameters encompassed CTT, RTT, TTP, vDRF, pDRF, RTT-CTT, absolute difference in vDRF as well as in pDRF, grade of pelvicalyceal dilation, pelvicalyceal AP diameter (mm), corticomedullary differentiation, cortical thinning, renal enhancement and excretion. We performed the statistical analysis for the whole sample counting each kidney as a separate unit (n=70) and repeated it, splitting the analysis based on the presence of pelvicalyceal dilation (pelvicalyceal dilation, n=40, and no pelvicalyceal dilation, n=30). Mann-Whitney, chi-square or Fisher tests were performed to evaluate the difference of each fMRU parameters between kidneys with and without pelvicalyceal dilation. P-values of less than 0.05 were considered significant.

Fig. 1 3-D T1-weighted gradient echo sequence with fat saturation (**a**) and b=0 axial image (**b**) in a 9-year-old-boy. The regions of interest of the right (blue) and left (green) renal parenchyma were exported from the clinical functional MR urography analysis (**a**) and loaded semiautomatically over the diffusion-weighted imaging (DWI) data (**b**)
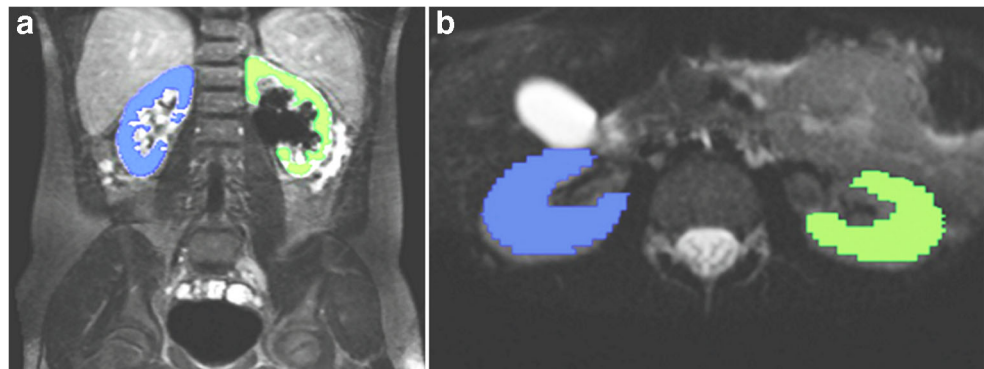
Results

Renal ADC correlation and age

ADC increases with age (R^2=0.154, P=0.001) in the 70 kidneys. Splitting the analyses based on the presence of pelvicalyceal dilation, ADC increases with age in the 30 kidneys without pelvicalyceal dilation (R^2=0.363, P<0.001); however, renal ADC does not correlate with age in the 40 kidneys with pelvicalyceal dilation (R^2=0.053, P=0.161) (Fig. 2).

Distribution of qualitative and quantitative parameters of fMRU

Table 1 summarizes the distribution of the fMRU qualitative parameters. The 30 kidneys without pelvicalyceal dilation had normal corticomedullary differentiation, cortical thickness, renal enhancement and excretion. Of the 40 kidneys with pelvicalyceal dilation, 15.0% had severe (Grade 5) pelvicalyceal dilation, 32.5% had decreased corticomedullary differentiation, 15.0% had severe cortical thinning, 2.5% had absent renal enhancement and 12.5% had absent excretion. The distribution of these qualitative parameters was statistically different between kidneys without and with pelvicalyceal

dilation (P<0.021). Table 2 shows the median and range of the fMRU quantitative parameters. The transit times and the difference between RTT-CTT are longer in the kidneys with pelvicalyceal dilation (P<0.026). Even though the median of the TTP was longer in the group with pelvicalyceal dilation, it was only marginally significant (P=0.060). The differential renal functions were statistically greater in the kidneys without pelvicalyceal dilation (P<0.005). As expected, the pelvicalyceal diameters were significantly greater in the group with pelvicalyceal dilation (P<0.001).

Correlation of fMRU and ADC

As shown in Table 3, renal ADC does not correlate with any of the morphological and fMRU parameters in the whole sample analysis or in each individual group analysis (P>0.070). The median ADC of kidneys without pelvicalyceal dilation was 3.73×10^{-3} mm^2/s (range: 2.78–5.37$\times10^{-3}$ mm^2/s) and the median ADC of kidneys with pelvicalyceal dilation was 3.82×10^{-3} mm^2/s (range: 2.70–5.70$\times10^{-3}$ mm^2/s). Figure 3 shows the absence of correlation of renal ADC and CTT and calyceal AP diameter.

In children with unilateral pelvicalyceal dilation, the median absolute difference of vDRF was 7.7% (range: 0.5–43.9%) and the median absolute difference of pDRF was 7.1% (range: 0.2–53.7%). There was no correlation of ADC and the absolute differences of vDRF or pDRF (P>0.332).

Discussion

The renal ADC values do not appear to correlate with any morphological (grade of pelvicalyceal dilation, cortical thinning, corticomedullary differentiation and pelvicalyceal AP diameters) or functional (renal enhancement, excretion, CTT, RTT, RTT-CTT, TTP, vDRF, pDRF, and absolute differences vDRF and pDRF) findings of fMRU in children with pelvicalyceal dilation. In addition, ADC increases with age in kidneys without pelvicalyceal dilation; however, no correlation was found between age and ADC in kidneys with pelvicalyceal dilation.

As previously reported by Jones and Grattan-Smith [13] and Delgado et al. [14], ADC increases with age in a healthy cohort of children, particularly in the first 2 years. In our cohort, the slope of the correlation with age and ADC was not particularly greater in the first 2 years. This can be explained by the small sample size of those younger than 2 years of age (n=8) and the heterogeneity of the morphology and function of the group. The ADC increase with age in children is not well understood as microstructural diffusivity changes and renal perfusion changes of the developing kidney occur at the same time. There are various reasons why renal ADC does not correlate with age in kidneys with
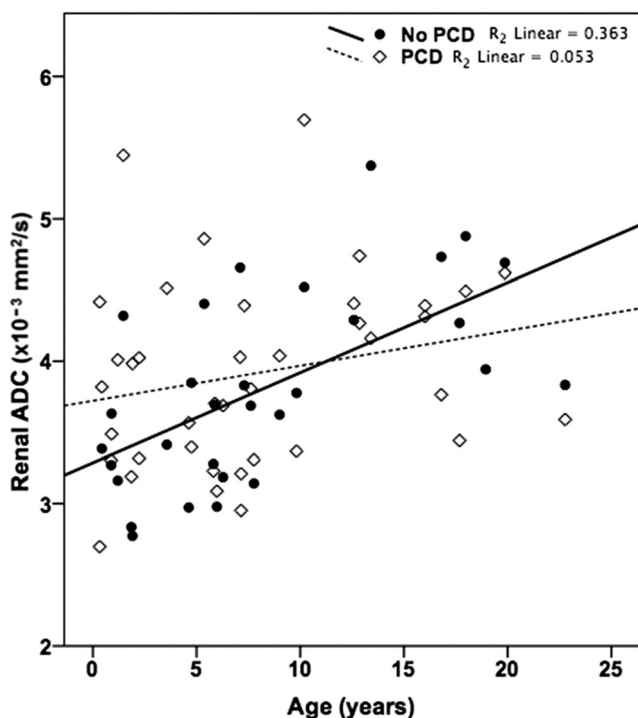

Fig. 2 Correlation between renal apparent diffusion coefficient (ADC) and age. Renal ADC increases with age in the 30 kidneys without pelvicalyceal dilation (PCD) (R^2=0.363, P<0.001); however, renal ADC does not correlate with age in the 40 kidneys with PCD (R^2=0.053, P=0.161)

Table 1 Distribution of qualitative parameters of *f*MRU based on pelvicalyceal dilation

fMRU parameter		No pelvicalyceal dilation (*n*=30)	Pelvicalyceal dilation (*n*=40)	*P* value*
Grade of pelvicalyceal dilation	No dilation (Grades 1 and 1-2)	30 (100%)	0 (0%)	<0.001
	Grade 3	0 (0%)	17 (42.5%)	
	Grade 4	0 (0%)	17 (42.5%)	
	Grade 5	0 (0%)	6 (15.0%)	
Corticomedullary differentiation	Normal	30 (100%)	27 (67.5%)	<0.001
	Decreased	0 (0%)	13 (32.5%)	
Cortical thinning	No cortical thinning	30 (100%)	17 (42.5%)	<0.001
	Mild	0 (0%)	10 (25.0%)	
	Moderate	0 (0%)	7 (17.5%)	
	Severe	0 (0%)	6 (15.0%)	
Renal enhancement	Normal	30 (100%)	29 (72.9%)	0.021
	Decreased	0 (0%)	10 (25.0%)	
	Absent	0 (0%)	1 (2.5%)	
Excretion	Normal	30 (100%)	11 (27.5%)	<0.001
	Decreased-no clinically relevant	0 (0%)	15 (37.5%)	
	Decreased-clinically relevant	0 (0%)	9 (22.5%)	
	Absent	0 (0%)	5 (12.5%)	

*Chi-square or Fisher exact test were performed between the categorical variables (presence of pelvicalyceal dilation vs. fMRU parameter)

fMRU functional MR urography

pelvicalyceal dilation. First, in kidneys with pelvicalyceal dilation there is a distortion in morphology and function of the renal parenchyma. This group also encompasses different degrees of pelvicalyceal dilation, parenchymal damage or dysplasia, and restricted renal function. Second, the effect of the obstruction in the developing kidney is variable, and it depends on individual factors such as time of onset, location and degree of obstruction [30]. Third, kidneys with dilated parenchyma are prone to motion artifacts, have thinner ROI and reduced accuracy of ROI placement. These factors predispose the ROIs to volume averaging with surrounding tissues. Fourth, kidneys with similar pelvicalyceal morphology may have different pressure within the renal pelvis and parenchyma due to variability between the degree of obstruction, urine production, impaired outflow, and pelvic size and distensibility. The latter may be due to different ratios between collagen and smooth muscle tissue [31]. Normal pressure can be achieved with an adequate balance of these factors; however, the loss of balance can produce transient or

Table 2 Median and range of quantitative *f*MRU parameters based on pelvicalyceal dilation

Parameters	Median (range)		*P* value*
	No pelvicalyceal dilation (*n*=30)	Pelvicalyceal dilation (*n*=40)	
CTT (s)	140 (99–199)	160 (99–9,120)	0.026
RTT (s)	180 (119–326)	509 (130–9,593)	<0.001
RTT-CTT (s)	30 (0–142)	286 (0–9,179)	<0.001
TTP (s)	150 (120–224)	170 (90–919)	0.060
vDRF (%)	52.9 (43.9–81.7)	47.7 (18.3–56.1)	<0.001
pDRF (%)	53 (31.0–72.0)	47.9 (28–69)	0.005
Intrapelvic diameter (mm)	6.8 (2.5–14.0)	24.0 (7.3–64.0)	<0.001
Calyceal diameter (mm)	2.0 (1.0–6.0)	12.5 (3.0–40.0)	<0.001

*Mann-Whitney test

CTT calyceal transit time, *fMRU* functional magnetic resonance urography, *pDRF* Patlak differential renal function, *RTT* renal transit time, *TTP* time-to-peak, *vDRF* volumetric differential renal function

Table 3 Correlation of renal apparent diffusion coefficient (ADC) values and *f*MRU parameters using hierarchical regressions controlling for age

| *f*MRU parameter	ADC correlation with *f*MRU parameters controlling age (*P* value)		
	Whole sample (*n*=70)	No pelvicalyceal dilation (*n*=30)	Pelvicalyceal dilation (*n*=40)
Grade of pelvicalyceal dilation	0.424	N/A	0.092
Corticomedullary differentiation	0.239	N/A	0.417
Cortical thinning	0.108	N/A	0.108
Renal enhancement	0.929	N/A	0.802
Excretion	0.385	N/A	0.754
Intrapelvic diameter (mm)	0.104	0.422	0.213
Calyceal diameter (mm)	0.227	0.597	0.367
CTT (s)	0.504	0.960	0.637
RTT (s)	0.944	0.610	0.831
RTT-CTT (s)	0.609	0.482	0.456
TTP (s)	0.145	0.432	0.096
vDRF (%)	0.474	0.130	0.070
pDRF (%)	0.124	0.133	0.717

CTT Calyceal transit time, *fMRU* functional MR urography, *pDRF* Patlak differential renal function, *RTT* renal transit time, *TTP* time-to-peak, *vDRF* volumetric differential renal function

permanent increase in pelvic pressure and therefore microstructural renal impairment that may not be visible on imaging [32].

Contradictory results have been reported regarding the usefulness of renal ADC values in evaluating pelvicalyceal dilation. Our study showed results conflicting with several authors who have proposed that renal ADC value has a potential correlation with renal function, showing lower ADC values with a decrease in GFR. Toyoshima et al. [15] found a positive correlation between ADC values and GFR in hydronephotic kidneys measured by scintigraphy; this study was done in adults with multiple causes of hydronephrosis. Müller et al. [33] described a decrease in renal ADC values 1-r post-ureteral obstruction in pigs. Kalayci et al. [16] reported that adult kidneys with chronic pelvicalyceal dilation, from benign or malignant etiology, had lower ADC values in comparison to normal controls. Xu et al. [34] reported that ADC may be useful in detecting tubulointerstitial injury, including atrophy and fibrosis. Lin et al. [22] evaluated the renal ADC in kidneys with UPJ obstruction in a pediatric population (age range: 5 months to 3 years) and compared it with their GFR, measured by scintigraphy. They reported that hydronephrotic kidneys with renal failure or decompensated renal function had lower renal ADC values than the contralateral kidneys or the control group. However, their analysis did not control the age factor in relation to the ADC value and GFR. GFR and renal ADC values increase with age, particularly in the first 2 years of life [13, 35]. Several authors have found no difference in the renal ADC values between the dilated and the non-dilated kidneys in adults with unilateral ureteral obstruction and

Fig. 3 Scatterplots show the absence of renal apparent diffusion coefficient (ADC) correlation with calyceal transit time (CTT) in seconds (**a**) or calyceal AP diameter in mm (**b**). *PCD* pelvicalyceal dilation
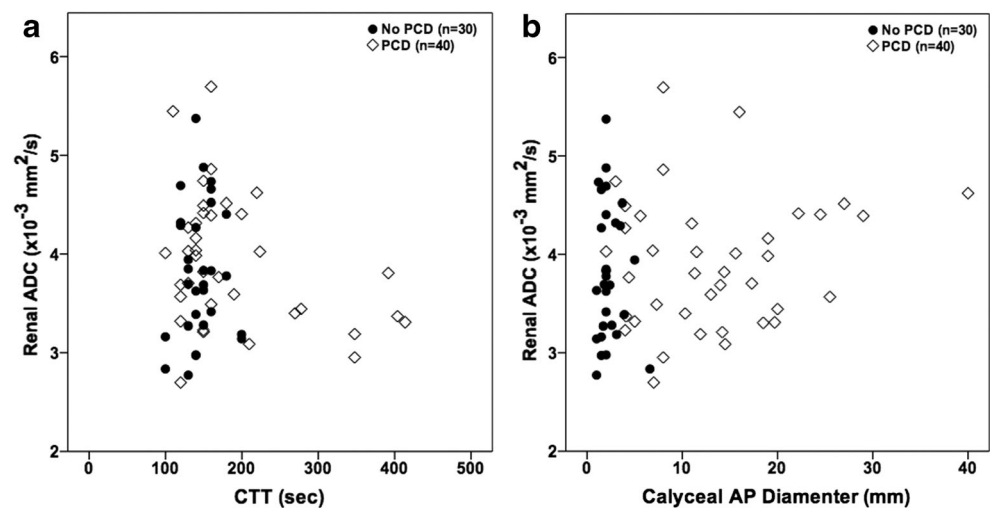
dilation of the collecting system [11, 20]. Macarini et al. [36] reported that kidneys with hydronephrosis have higher renal ADC values in comparison to normal kidneys. In our study, no difference was found. Kocyigit et al. [21] evaluated renal ADC in children with vesicoureteral reflux. They did not find correlation between renal ADC values and grade of vesicoureteral reflux or difference of ADC values with controls.

The role of fMRU in clearly differentiating which kidneys with suspected UPJ obstruction are really obstructed or in predicting postsurgical outcome is still evolving [37]. Still, the comprehensive information from qualitative evaluation of the dynamic images and fMRU quantitative results, particularly in aggregate, are useful. There is high variability in the outcome of obstruction on the renal parenchyma based on the cause, the age of onset and the balance between the degree of obstruction, urine production, pelvic reservoir, and vasoactive factors and cytokines. Similar fMRU findings can be found in kidneys with or without active obstruction. Pelvicalyceal dilation can occur in the absence of urinary obstruction. Dilated renal pelvis or calyces do not necessarily mean that the renal function is decreased or the kidney is obstructed [38]. Intrinsic individual factors that may not be detected by fMRU have the potential to alter the microstructural organization and therefore the diffusivity of the kidney.

We transferred the fMRU ROIs to the DWI data to be sure we were comparing the same structural location in the functional post-processing analysis and the ADC maps. The ROIs were placed on the whole parenchyma because the renal parenchyma had a heterogeneous ADC map and it was not possible to differentiate the medulla from the cortex as found in multiple studies [15, 16, 18–20, 22, 36, 39]. Renal ADC has been proven to be a reproducible measurement [11, 19, 36, 40]; however, the comparison of absolute ADC values with other published studies is not possible because it varies based on MR scanners, technique parameters, coils, magnetic fields, b-values, ADC calculation formulas, ROI placements, hydration states and diffusion encoding methods [40–42]. We included constant b-values and the same MR system as well as those scans with the standard prehydration and use of Lasix to avoid intrinsic variability of ADC values.

We advocate for the addition of a DWI sequence in the fMRU protocol due to its high diagnostic value in evaluating subtle parenchymal diseases, such as infection and hypercellular lesions. However, the analysis of the DWI sequence should focus on morphological interpretation of the DWI images and the ADC maps instead of the quantitative analysis of the ADC values. Our institutional protocol was updated based on these results. Instead of using 5 b-values (0, 200, 500, 800 and 1,000 s/mm^2), we reduced the imaging time by having only 3 b-values (0, 500 and 800 s/mm^2). This provides an adequate sequence to evaluate restriction patterns in the renal parenchyma due to infection [8–10] or tumor recurrence [4–6] that may not be identified on the conventional fMRU sequences; for example, Figure 4 shows a subtle recurrent Wilms tumor that was not identified on conventional sequences.

This study has several limitations related to its retrospective nature. The 30 kidneys without dilation in the patients with contralateral pelvicalyceal dilation may not entirely be free of pathology and may have microstructural and functional compensatory mechanisms that we could not assess. There is no histopathological correlation of the renal parenchyma. Creatinine levels are not routinely acquired in this patient population at our institution; therefore, we could not correlate renal ADC with GFR as several published data. The sample was heterogeneous and some kidneys had prior surgery. For the ROI placement, we assumed the patient does not move between the fMRU and DWI sequences. Any motion will cause the ROIs to be improperly placed. For that reason, we
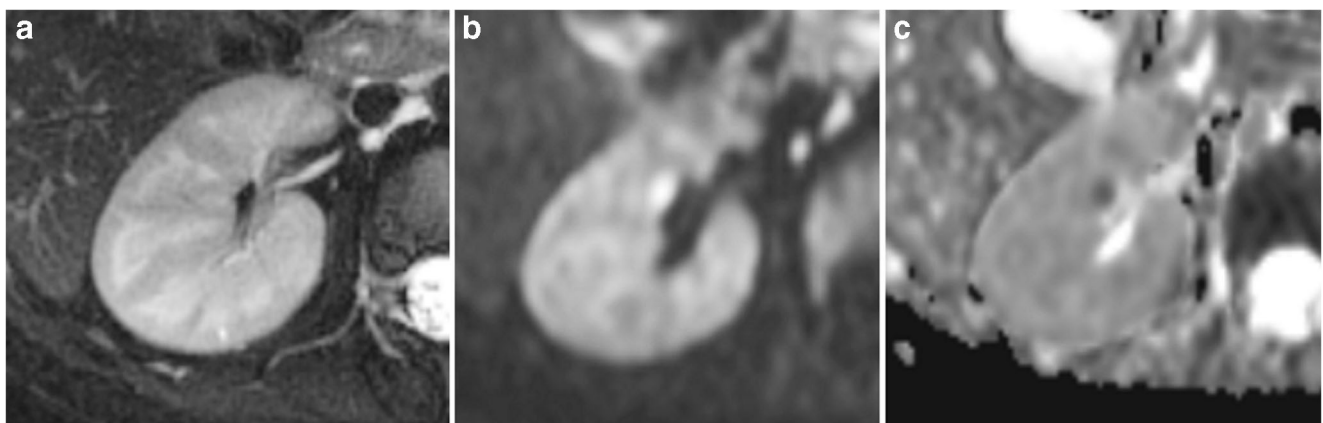

Fig. 4 Normal axial T2 high-spatial resolution image (**a**) in a 2-year-old boy with a history of Wilms tumor and left nephrectomy. Focal parenchymal lesion with restricted diffusion pattern with high signal intensity on the b=1,000 image (**b**) and low signal intensity on the apparent diffusion coefficient (ADC) map (**c**). The imaging findings are consistent with the final diagnosis of recurrent Wilms tumor confirmed histologically

were strict in the exclusion of the 37 cases with suboptimal position of the renal ROIs. However, there is a degree of subjectivity in such a selection. In the retrospective setting, not all technical scan parameters can be controlled. The large range of the slice thickness of the DWI sequences is such an example.

Conclusion

Our study demonstrated that renal ADC does not correlate with the morphological and functional results of fMRU changes in children with pelvicalyceal dilation with suspected or known UPJ obstruction.

Compliance with ethical standards

Conflicts of interest None

References

1. Hagmann P, Jonasson L, Maeder P et al (2006) Understanding diffusion MR imaging techniques: from scalar diffusion-weighted imaging to diffusion tensor imaging and beyond. Radiographics 26:S205–S223
2. Qayyum A (2009) Diffusion-weighted imaging in the abdomen and pelvis: concepts and applications. Radiographics 29:1797–1810
3. Saremi F, Knoll AN, Bendavid OJ et al (2009) Characterization of genitourinary lesions with diffusion-weighted imaging. Radiographics 29:1295–1317
4. Razek AA, Farouk A, Mousa A, Nabil N (2011) Role of diffusion-weighted magnetic resonance imaging in characterization of renal tumors. J Comput Assist Tomogr 35:332–336
5. Squillaci E, Manenti G, Cova M et al (2004) Correlation of diffusion-weighted MR imaging with cellularity of renal tumours. Anticancer Res 24:4175–4179
6. Lassel EA, Rao R, Schwenke C et al (2014) Diffusion-weighted imaging of focal renal lesions: a meta-analysis. Eur Radiol 24:241–249
7. Zhang H, Gan Q, Wu Y et al (2016) Diagnostic performance of diffusion-weighted magnetic resonance imaging in differentiating human renal lesions (benignity or malignancy): a meta-analysis. Abdom Radiol (NY) 41:1997–2010
8. De Pascale A, Piccoli GB, Priola SM et al (2013) Diffusion-weighted magnetic resonance imaging: new perspectives in the diagnostic pathway of non-complicated acute pyelonephritis. Eur Radiol 23:3077–3086
9. Faletti R, Cassinis MC, Fonio P et al (2013) Diffusion-weighted imaging and apparent diffusion coefficient values versus contrast-enhanced MR imaging in the identification and characterisation of acute pyelonephritis. Eur Radiol 23:3501–3508
10. Henninger B, Reichert M, Haneder S et al (2013) Value of diffusion-weighted MR imaging for the detection of nephritis. ScientificWorldJournal 2013:348105
11. Thoeny HC, De Keyzer F, Oyen RH, Peeters RR (2005) Diffusion-weighted MR imaging of kidneys in healthy volunteers and patients with parenchymal diseases: initial experience. Radiology 235:911–917
12. Abou-El-Ghar ME, El-Diasty TA, El-Assmy AM et al (2012) Role of diffusion-weighted MRI in diagnosis of acute renal allograft dysfunction: a prospective preliminary study. Br J Radiol 85:e206–e211
13. Jones RA, Grattan-Smith JD (2003) Age dependence of the renal apparent diffusion coefficient in children. Pediatr Radiol 33:850–854
14. Delgado J, Berman JI, Maya C et al (2019) Pilot study on renal magnetic resonance diffusion tensor imaging: are quantitative diffusion tensor imaging values useful in the evaluation of children with ureteropelvic junction obstruction? Pediatr Radiol 49:175–186
15. Toyoshima S, Noguchi K, Seto H et al (2000) Functional evaluation of hydronephrosis by diffusion-weighted MR imaging. Relationship between apparent diffusion coefficient and split glomerular filtration rate. Acta Radiol 41:642–646
16. Kalayci TO, Apaydin M, Sonmezgoz F et al (2014) Diffusion-weighted magnetic resonance imaging findings of kidneys with obstructive uropathy: differentiation between benign and malignant etiology. ScientificWorldJournal 2014:980280
17. Fukuda Y, Ohashi I, Hanafusa K et al (2000) Anisotropic diffusion in kidney: apparent diffusion coefficient measurements for clinical use. J Magn Reson Imaging 11:156–160
18. Xu Y, Wang X, Jiang X (2007) Relationship between the renal apparent diffusion coefficient and glomerular filtration rate: preliminary experience. J Magn Reson Imaging 26:678–681
19. Xu X, Fang W, Ling H et al (2010) Diffusion-weighted MR imaging of kidneys in patients with chronic kidney disease: initial study. Eur Radiol 20:978–983
20. Bozgeyik Z, Kocakoc E, Sonmezgoz F (2009) Diffusion-weighted MR imaging findings of kidneys in patients with early phase of obstruction. Eur J Radiol 70:138–141
21. Kocyigit A, Bayram R, Yuksel S et al (2014) Diffusion weighted magnetic resonance imaging of kidneys in children with vesicoureteral reflux. Eur J Radiol 83:e56–e60
22. Lin F, Li Z, Gan Y et al (2014) Relationship between renal apparent diffusion coefficient values and glomerular filtration rate in infants with congenital hydronephrosis. Biosci Trends 8:274–279
23. Kim JW, Lee CH, Yoo KH et al (2016) Intravoxel incoherent motion magnetic resonance imaging to predict vesicoureteral reflux in children with urinary tract infection. Eur Radiol 26:1670–1677
24. Khrichenko D, Darge K (2010) Functional analysis in MR urography - made simple. Pediatr Radiol 40:182–199
25. Darge K, Higgins M, Hwang TJ et al (2013) Magnetic resonance and computed tomography in pediatric urology: an imaging overview for current and future daily practice. Radiol Clin N Am 51:583–598
26. Riccabona M, Avni FE, Blickman JG et al (2008) Imaging recommendations in paediatric uroradiology: minutes of the ESPR workgroup session on urinary tract infection, fetal hydronephrosis, urinary tract ultrasonography and voiding cystourethrography, Barcelona, Spain, June 2007. Pediatr Radiol 38:138–145
27. Delgado J, Bedoya MA, Adeb M et al (2015) Optimizing functional MR urography: prime time for a 30-minutes-or-less fMRU. Pediatr Radiol 45:1333–1343
28. O'Halloran RL, Holmes JH, Altes TA et al (2007) The effects of SNR on ADC measurements in diffusion-weighted hyperpolarized He-3 MRI. J Magn Reson 185:42–49
29. Chandarana H, Lee VS, Hecht E et al (2011) Comparison of biexponential and monoexponential model of diffusion weighted imaging in evaluation of renal lesions: preliminary experience. Investig Radiol 46:285–291
30. Chevalier RL (1995) Effects of ureteral obstruction on renal growth. Semin Nephrol 15:353–360

31. Kim WJ, Yun SJ, Lee TS et al (2000) Collagen-to-smooth muscle ratio helps prediction of prognosis after pyeloplasty. J Urol 163: 1271–1275

32. Grattan-Smith JD (2008) MR urography: anatomy and physiology. Pediatr Radiol 38:S275–S280

33. Muller MF, Prasad PV, Bimmler D et al (1994) Functional imaging of the kidney by means of measurement of the apparent diffusion coefficient. Radiology 193:711–715

34. Xu X, Palmer SL, Lin X et al (2017) Diffusion-weighted imaging and pathology of chronic kidney disease: initial study. Abdom Radiol (NY) 43:1749–1755

35. Saint-Faust M, Boubred F, Simeoni U (2014) Renal development and neonatal adaptation. Am J Perinatol 31:773–780

36. Macarini L, Stoppino LP, Milillo P et al (2010) Diffusion-weighted MRI with parallel imaging technique: apparent diffusion coefficient determination in normal kidneys and in nonmalignant renal diseases. Clin Imaging 34:432–440

37. Grattan-Smith JD, Jones RA (2008) MR urography: technique and results for the evaluation of urinary obstruction in the pediatric population. Magn Reson Imaging Clin N Am 16: 643–660 viii-ix

38. Alberti C (2012) Congenital ureteropelvic junction obstruction: physiopathology, decoupling of tout court pelvic dilatation-obstruction semantic connection, biomarkers to predict renal damage evolution. Eur Rev Med Pharmacol Sci 16:213–219

39. Toya R, Naganawa S, Kawai H, Ikeda M (2010) Correlation between estimated glomerular filtration rate (eGFR) and apparent diffusion coefficient (ADC) values of the kidneys. Magn Reson Med Sci 9:59–64

40. Bilgili MY (2012) Reproducibility of apparent diffusion coefficients measurements in diffusion-weighted MRI of the abdomen with different b values. Eur J Radiol 81:2066–2068

41. Donati OF, Chong D, Nanz D et al (2014) Diffusion-weighted MR imaging of upper abdominal organs: field strength and intervendor variability of apparent diffusion coefficients. Radiology 270:454–463

42. Zhang JL, Sigmund EE, Chandarana H et al (2010) Variability of renal apparent diffusion coefficients: limitations of the monoexponential model for diffusion quantification. Radiology 254:783–792